# PULSED PLASMACHEMISTRY OF $CO_X$, $NO_X$, $SO_X$

**G.P. Berezina, I.N. Onishchenko, V.S. Us**

*NSC Kharkov Institute of Physics & Technology*
*Academic St. 1, Kharkov 310108, Ukraine*
*onish@kipt.kharkov.ua*

**Abstract –** The pulsed spark discharge at atmosphere pressure has been considered as a suitable tool for plasma chemistry of $CO_X$, $NO_X$, and $SO_X$. The multi-spark electric discharge, "dancing" between a set of eagles and a plate was used for the treatment of a considerable gas volume. The theoretical and experimental investigations have been performed to dissociate the gases mentioned above. In particular the percentage of $CO_X$ dissociation above 30% has been achieved in accordance with the theoretical evaluations.

## 1. Introduction

We define the term "pulsed plasmachemistry" as some chemical phenomena in non-equilibrium plasma, produced by a pulsed electric discharge at atmospheric pressure. Pulsed mode of operation is caused by the fact that at high pressure conditions needed for large amount gas treatment in a considerable simple technology the only possible mean is a pulsed discharge at gas breakdown at atmospheric pressure [1]. During short temporal interval it forms optimum energy distribution function of plasma electrons, suitable for the excitation of the energy levels needed for efficient chemical reactions. Calculated time duration of the pulse can be provide by external electric chain [1] or as it follows from this presentation it can be obtain due to self-consistent processes in the discharge at DC applied voltage or/and in RC-relaxation scheme. To increase the products yield two measures were undertaken. Firstly the repetitive mode was used proceed from the requirements that the pulse off-duty factor should provide the products buildup. Secondly traveling discharge "jumping" and "dancing" in and through over the interelectrodes space was realized in the following geometry configuration: a set of eagle + plane. At last for processing enhancement the direct-flow regime can occur useful.

## 2. Theoretical studies of gas dissociation in the pulsed travelling gas discharge

The plasma-chemical reactor (PCR) is a chamber filled with a working gas, where a discharge is ignited between the electrodes, to which a certain potential difference is applied. The discharge type and the character of plasma-chemical reactions are dependent on the electrode geometry, voltage value and character (direct, pulsed, one- or two-polar), and on the gas mixture composition. The PCR can operate at atmospheric pressure in the direct-flow regime in order to be able to replace the mixture in the process of its chemical transformation.

In view of all these factors, the following scheme was used in the theoretical model:

- Locally, considering the $E/N$ ratio value ($E$ is the electric intensity, $N$ is the neutral gas particle density) and the chemical reactions taking place in the system with the participation of electrons, the electron energy distribution function is calculated $f_e(\varepsilon)$.
- Based on the analysis of the processes of ionization, attachment, detachment and recombination established are the character of conductivity and the type of principal current carriers in the discharge, their concentration as a function of the power input in the discharge.
- Proceeding from the calculated concentrations of current carriers and the electron distribution functions, and also using the known-from-literature cross-sections for basic processes, we have chosen the energy input channels by which the plasma-chemical reactions take place. After that, a kinetic consideration is given to all possible plasma-chemical reactions. The peak values of reaction product concentrations the time for attaining these peak values and the time of product buildup were determined in a similar way. The dynamics of basic plasma-chemical reactions with time was numerically investigated using the PC.
- The direct-flow conditions are analyzed by the equation of continuity with due account of the processes of transport and diffusion.

### 2.1 The distribution function

To obtain the distribution function that sets in at a given $E/N$ value, we restrict ourselves to the kinetics of the following reactions:

1) excitation of vibration levels of $CO_2$ molecules by an electron impact

$$CO_2 + e \rightarrow CO_2(v) + e', \quad \varepsilon_1 = 0.083 \text{ eV}; \quad (1)$$

2) dissociation of the $CO_2$ molecule into the $CO$ molecule and the $O$ atom

$$CO_2 + e \rightarrow CO + O + e, \quad \varepsilon_2 = 5.5 \text{ eV}; \quad (2)$$

3) dissociation of $CO_2$ with the attachment of electron to the oxygen atom

$$CO_2 + e \rightarrow CO + O^-, \quad \varepsilon_3 = 4.0 \text{ eV}; \quad (3)$$

4) ionization of the $CO_2$ molecule by the electron impact

$$CO_2 + e \rightarrow CO_2^+ + 2e, \quad \varepsilon_4 = 13.8 \text{ eV}. \quad (4)$$

The energy value expended per event is given for each reaction. The distribution function $f_e(\varepsilon)$ is derived from the stationary homogeneous Boltzmann equation in the two-body approximation (this procedure is given

elsewhere); it describes the electron energy distribution at a given $E/N$, taking into account elastic collisions; oscillational, rotational and translational kinetics and the kinetics of the above-mentioned processes.

For $E/N = 50$ Td, that corresponds to the conditions of our experiments ($E =$ 12.5 kV/cm at $CO_2$ pressure of 1 atm.), the distribution function is the double doorstep non-Maxwell one with the mean electron energy 2 eV. For this electron energy vibration excitation cross-section is considerable, while this energy is significantly lower than the $CO_2$ dissociation, dissociative attachment, and ionization energy. The cascade vibrational-level pumping results in attaining the level of dissociation. For estimation, the coefficient $k = \varepsilon_2/\varepsilon_1 = 5.5/0.083 = 66$ was introduced. It reduces the effective cross section for vibrational level excitation in the calculations.

The derived distribution function $f_e$ makes it possible to obtain the coefficients of reactions (1–4) as a parameter $\langle \sigma_i v \rangle$ averaged over the distribution function

$$k_i = \langle \sigma_i v \rangle = \int \sigma_i \varepsilon f(\varepsilon) d\varepsilon . \qquad (5)$$

For determination of the electron density in the discharge, it is of importance to know the directional (drift) velocity of electrons:

$$\langle v_x \rangle = \int v_x \sqrt{\varepsilon} f(\varepsilon) d\varepsilon . \qquad (6)$$

### 2.2 Electron concentration in the discharge

The current transport is effected by ions or electrons, depending on the discharge geometry ("needle-plane", "plane-plane", the interelectrode spacing, transverse dimensions), the electrode material and, particularly, on the type of discharge (corona, glow, spark or arc). In the case of electronic current transport, the local electron density can be calculated from the current density:

$$j = e n_e v_x \qquad (7)$$

In the case of current transport by ions, the problems becomes complicated because it appears necessary to determine, first, the density ratios of electrons, negative and positive ions; and, secondly, the ion mobility.

The second problem in the calculations of electron density is to take into account the two-dimensionality and the inhomogeneity of the problem in the case of "needle-plane" geometry. With this geometry, the greatest $E/N$ value is attained in the vicinity of the needle, where the ionization processes dominate over the inverse processes such as recombination, attachment, and diffusion. At a negative needle potential this situation is typical of the sphere with a center near the needle, on the surface of which the processes of production and loss of electrons are balanced. Outside this sphere the current transport is realized only by negative ions and electrons, whereas inside the sphere - by positive ions and electrons. The current in the direction of the needle is generated by positive ions only. On the boundary sphere, whose radius is determined by the $E^*(r)/N$ value corresponding to the equilibrium between recombination or attachment and ionization, the current transport is determined only by electrons. For the same reduced field $E^*/N$ value, we derive the drift velocity of electrons $v_x^*$, that permits the calculation of the electron density

$$n_e^* = \frac{j}{e v_x^*} = \frac{Q}{e E^* v_x^*} , \qquad (8)$$

where $Q$ is the specific power input in the discharge.

To find the coefficients of the chemical reaction of $CO_2$ molecule dissociation, the average value of the electron density $\overline{n}_e$ should be found. This task is much more complicated, it is solved separately elsewhere. Below for $\overline{n}_e$ estimation we shall use $n_e^*$ from eq. (8).

At a positive needle polarity, the current transport to the needles is provided by electrons (in the case of electronegative gas components, by negative ions, too) that arise owing to gas ionization in the region of high $E/N$ values near the needle. In consequence of lower mobility as compared to electron, the positive ions are built up in the vicinity of the needle. The positive space charge significantly changes the potential distribution between the electrodes and essentially affects the value of ion current to the negative electrode (plane). However, in this case, too, the concentration of electrons that plays an important role in the $CO$ production, especially at the initial stage, when the concentration of components participating in the reactions is still insignificant and is derived from eq. (8).

### 2.3 Kinetic equations of plasma-chemical reactions

The average electron energy, the electron drift velocity, and in accordance with the specific power input $Q$ the electron density have been found in previous sections. This allows to calculate the $CO_2$ dissociation coefficient, whose value depends on the specific power $Q$, as

$$k_1(Q) = \sum_i n_e^i \langle \sigma_i v \rangle , \qquad (9)$$

where the averaging is performed over the derived distribution function for all the processes with the cross sections $\sigma_i$, the main of which for the experimental conditions considered are the vibrational level excitation resulting in the $CO_2$ dissociation and the direct $CO_2$ dissociation due to electron impact.

The scheme of chemical reactions in the PCR to produce $CO$ from $CO_2$ in the discharge involves the following reactions [2-4]:

1) $CO_2$ dissociation by electron impact with the dissociation coefficient $k_1$:

$$CO_2 + e \rightarrow CO + O + e ; \qquad (10)$$

2) $CO$ production using atomic oxygen

$$CO_2 + O \rightarrow CO + O_2 , \qquad (11)$$

$$k_2 = 2 \cdot 10^{-16} \text{ cm}^3/\text{mole} \cdot \text{s};$$

3) reaction of inverse oxidation of $CO$ into $CO_2$ by atomic oxygen $O$ on the oxygen $O_2$ molecule

$$CO + O + O_2 \rightarrow CO_2 + O_2, \quad (12)$$
$$k_3 = 3.6 \cdot 10^{-33} \text{ cm}^6/\text{s};$$

4) reaction of inverse oxidation of $CO$ into $CO_2$ by atomic oxygen $O$ on the $CO_2$ molecule

$$CO + O + CO_2 \rightarrow 2CO_2, \quad (13)$$
$$k_4 = 7.2 \cdot 10^{-36} \text{ cm}^6/\text{s};$$

5) reaction of atomic-to-molecular oxygen conversion on the $CO_2$ molecule

$$O + O + CO_2 \rightarrow O_2 + CO_2, \quad (14)$$
$$k_5 = 5.8 \cdot 10^{-32} \text{ cm}^6/\text{s}.$$

6) reaction of molecular-to-atomic oxygen conversion under the action of the electron impact

$$O_2 + e \rightarrow e + O + O, \quad (15)$$
$$k_6 = 10^{-9} \text{ cm}^3/\text{s}$$

For the one-dimensional case from the continuity equations with the corresponding kinetic terms we derive a set of coupled kinetic equations that describes reactions (10-15):

$$\frac{dn_{CO}}{dt} = k_1(Q)N_{CO_2} + k_2 n_O N_{CO_2} - k_3 n_{CO} n_O n_{O_2} - k_4 n_{CO} n_O N_{CO_2}, \quad (16)$$

$$\frac{dn_O}{dt} = k_1(Q)N_{CO_2} - k_2 n_O N_{CO_2} - k_3 n_{CO} n_O n_{O_2} - k_4 n_O n_{CO} N_{CO_2} - k_5 n_O^2 N_{CO_2} \quad (17)$$

$$\frac{dN_{CO_2}}{dt} = -\frac{dn_{CO}}{dt} \quad (18)$$

$$\frac{dn_{O_2}}{dt} = k_2 n_O N_{CO_2} + k_5 n_O^2 N_{CO_2} - k_6 n_{O_2} n_e \quad (19)$$

where $n_i$ is the particle density of the $i$-th component.

The set of eqs. (16-19) was solved numerically. For the analytical analysis, we restrict ourselves to the approximation of essential excess of $k_1$, $k_3$ and $k_5$ components, that is valid at small time intervals, and also at arbitrary time intervals with low production, i.e., $n_{CO}, n_O << N_{CO_2}$. We also note that the $CO$ production by electron excitation prevails over the dissociation in reaction with the atomic oxygen as far as to the concentrations $n_O$ that meets the conditions

$$n_O < \bar{n}_e \frac{\langle \sigma_i v \rangle}{k_2}. \quad (20)$$

In this approximation and taking into account that $n_O << n_{CO}$, $n_{O_2} \approx 1/2\, n_{CO}$, eqs. (16-17) take the form

$$\frac{dn_{CO}}{dt} = k_1(Q)N_{CO_2} - \frac{1}{2}k_3 n_{CO}^2 n_O, \quad (21)$$

$$\frac{dn_O}{dt} = k_1(Q)N_{CO_2} - k_5 n_O^2 N_{CO_2}. \quad (22)$$

For the steady-state case ($\frac{dn_i}{dt} = 0$), we find the estimation of maximum $O$ and $CO$ production values:

$$n_O^{max} = \sqrt{\frac{k_1}{k_5}}, \quad (23)$$

$$n_{CO}^{max} = \sqrt{\frac{2\sqrt{k_1 k_5} N_{CO_2}}{k_3}}. \quad (24)$$

The point of importance that follows from (24) is the enhancement in the $CO$ production with an increase in the power input in the discharge. Naturally, in this case, the conditions of both the oscillation level excitation and dissociation must be held, i.e., the conditions for retaining the $E/N$ value that determines the electron energy distribution function. The time of reaching the steady-state value is determined as a ratio of the maximum concentration to the concentration growth rate:

$$\tau_i = \frac{n_i^{max}}{k_1 N_{CO_2}}. \quad (25)$$

For $O$ and $CO$ production, (25) gives the relations:

$$\tau_O = \frac{1}{\sqrt{k_1 k_5}} \frac{1}{N_{CO_2}}, \quad (26)$$

$$\tau_{CO} = \sqrt{\frac{2\sqrt{k_1 k_5}}{k_1^2 k_3 N_{CO_2}}}. \quad (27)$$

A low concentration of atomic oxygen (relative to the $CO$ concentration) and a quick reaching of a steady-state value are explained by a significant $k_5$ value of reaction (14). In this case, the balance of elements in accord with (10) is conserved. So, to an accuracy of $n_O/n_{CO} \approx 1\%$, the content of molecular oxygen $O_2$ produced in the discharge at $CO$ production from carbon dioxide $CO_2$ is half as that of $CO$. This is confirmed by experiments.

At essential production yields, when the condition (20) is not satisfied, the exact numerical solutions of eqs. (16-19) to determine the time dynamics of the components $CO$, $CO_2$, $O$ and $O_2$ were obtained numerically on PC.

The discharge was first ignited for the case of continuous steady-state input of power to the discharge. However, in a number of cases, e.g., for $CO_2$ at 1 atm it appears impossible to sustain the discharge with the required reduced electrical field $E/N$ ratio in order to obtain the optimum distribution function. As will be shown below, this challenge can be solved experimentally by going to the pulsed mode of operation, namely, to the travelling spark discharge. The potential difference between the electrodes should provide for the electrical breakdown of the gas under study, and the pulse duration should be rather small to preclude the development of arc discharge. The needed $E/N$ value is attained by the appropriate choice of voltage and interelectrode spacing. As demonstrated by our experiments, the "charging" current pulse duration is determined by a self-consistent

evolution of the discharge and makes $\tau_{ch} = 0.5$ μs with the current amplitude of tens of amperes (analogue of Trichel pulses [5]).

To determine the appropriate pulse length and the pulse repetition rate, two circumstances must be taken into account. First, the pulse length $\tau_{pul}$ should satisfy the conditions

$$\tau_{ch} < \tau_{pul} < \tau_a , \qquad (28)$$

where $\tau_a$ is the time of arc discharge development.

Secondly, the pulse off-duty factor should be such as to ensure the buildup of $CO$. To solve this problem, it is necessary to estimate the time of $CO$ production $\tau_{CO}$, the electron recombination time $\tau_e$, the time of atomic $O$-to-molecular $O_2$ oxygen relaxation or the $CO$ buildup time $\tau_b$, and also the time of $CO$-to-$CO_2$ relaxation on the oxidation by atomic oxygen $O$ (oxidation time $\tau_{CO}^R$). The pulse duration should not exceed the time needed for the concentration $n_{CO}$ to take the steady-state value:

$$\tau_{pul} < \tau_{CO} , \qquad (29)$$

because otherwise it would not be beneficial to bring a significant power into the discharge. The pulse repetition rate $f = 1/T$ should not be low in order to ensure the maximum energy input in the discharge and have an upper bound imposed by the needs of product buildup

$$T > \tau_{pul} + \tau_b . \qquad (30)$$

## 2. Experimental Set-up

Experiments on decomposition of $CO_2$, $NO_2$ and $SO_2$ in the pulsed discharge were carried out using the facility, shown in Fig. 1.

The cylindrical kovar glass vessel (*3*), whose ends are soldered with the flanges made from kovar (*2*, *6*), serves both gas-discharge chamber and the chemical reactor.

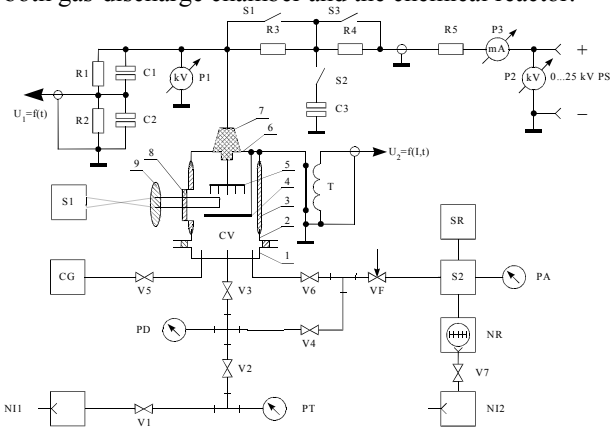


*Fig. 1. Plasma chemical reactor: CV - reactor chamber, CG - working gas chamber, NI1 - vacuum mechanical pump NVZ-20, NI2 - vacuum mechanical pump 2 NVR-5DM; NR - vacuum turbomolecular pump VMN-500; S1 - spectrograph DFS-452, S2 - mass-spectrometer MX7301, SR - two-coordinate self-recorder N-306, PD - deformation vacuum gauge; PA -ionization vacuum gauge, PT - thermal vacuum gauge; V1 ... V7 - straight-way valves, VF - metering valve, R1 ... R5 - resistors, C1 ... C3 - capacitors, P1, P2 - kilovoltmeters C96; T - transformer (Rogowsky belt). 1 - reactor bottom, 2 - lower flange of the reactor chamber, 3 - glass case of the chamber, 4 - lower electrode, 5 - upper electrode, 6 - upper flange of the chamber, 7 - insulator, 8 - quartz window, 9 - quartz lens.*

Along the axis of the vessel two insulated electrodes (*4*, *5*) were placed. The working volume of the reactor was $3.5 \cdot 10^{-3}$ m$^3$. The lower electrode was made from aluminum. It had a shape of a mushroom with a plane cap ($3.8 \cdot 10^{-2}$ m in diameter) and rounded borders. The upper electrode, movable along the axis, was a stainless steel rod, $8 \cdot 10^{-3}$ m diameter, with a conical end to ignite the arc discharge. For other case, it was a comb including seven copper wires ($5 \cdot 10^{-4}$ m diameter, each being $5 \cdot 10^{-3}$ m in length), that were soldered into the copper plate at an equal spacing $\cdot 10^{-3}$ m. The length of the comb correspondeds to the diameter of the lower electrode.

The electrodes of the discharge chamber are power supplied via ballast resistors from the controlled dc source having maximum power $W$=4 kW ($U_0$= 0-30 kV, $I_{max}$=150 mA). The discharge chamber design provided the conditions for igniting the discharge of three types: corona and arc discharges with a constant current, and the spark discharge at a repetitive pulsed mode of operation. For any type of discharge, the breakdown voltage of the discharge gap of the chamber is proportional to the interelectrode spacing and is inversely proportional to the gas pressure in the discharge gap.

The corona-discharge mode of operation is characterized by a high voltage across the discharge gap $U = U_0$ and a low current $I \le 1$ mA. At the arc-discharge mode of operation a considerable current $I \ge 15$ mA sets in at a comparatively low voltage $U = (0.1 \text{ to } 0.3)U_0$. The spark-discharge mode of operation was realized in the case when relaxation oscillations appeared in the electrodes circuit and their power supply. They approach a periodic sequence of pulses.

The two-coordinate self-recorder registered from mass-spectrometer the mass-spectra of initial and discharge-initiated products. The taken spectrum was used to calculate the percentage content of gas components.

## 4. Experimental Results

### 4.1 Carbon dioxide dissociation

To define the conditions of maximum extraction of $CO$ from $CO_2$ at a pressure of ~ 1 atm, three types of discharges were investigated: corona, arc and spark. The burning of discharges of these types in the reactor at all pressures (including the atmospheric pressure) can be sustained without any limit in time. Based on numerous experiments performed, we have established the type of atmospheric-pressure discharge that most completely meets the requirements of the task set. This is the spark discharge that is burning between the comb consisting of a few copper wires and a planar aluminum electrode. The

spark broke down the discharge gap without centering on any particular electrode, all the tips were participating in the process with equal probability, i.e., the spark was running from one tip over to the others. The interelectrode spacing was set in accordance with the applied voltage and ranged between (1.2 and 1.8)·$10^{-2}$ m. The power supply voltage was 20 to 25 kV, the breakdown voltage across the electrodes was 10 to 13 kV, the ballast resistance was $R_{bal} = 2.5$ MΩ.

As can be seen from Fig. 2 the content of carbon oxide $CO$ produced from $CO_2$ at optimum conditions of arc and spark discharges was about 3 to 4% (the corresponding time of production was 30 and 60 minutes).

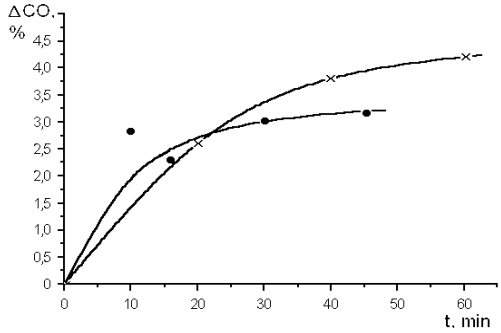


*Fig. 2. $CO$ production in arc (×) and spark (●) discharges.*

To optimize the process of production of $CO$, a capacitor of ~ 150 to 1000 pF was connected parallelly to the discharge gap. The capacitance value determined the charge time and, correspondingly, the spark frequency in the discharge gap, 0.3 kHz$\leq f \leq$ 1.2 kHz. Besides, the spark repetition rate was dependent on the interelectrode spacing and the power supply voltage.

The measurements have shown that the production of $CO$ at the repetitive mode increased by factors of 4 to 5 (see Fig. 3). In this case, the discharge parameters were: voltage $U = 25$ kV, pulse current $I \approx 80$ A, the current pulse length was 0.5·$10^{-6}$ sec with $I_{avr} \leq 10$ mA, interelectrode spacing $d = 1.3 \cdot 10^{-2}$ m, capacitor capacitance $C = 220$ pF, repetition frequency $f \sim 1$ kHz, $CO_2$ pressure 1 atm.

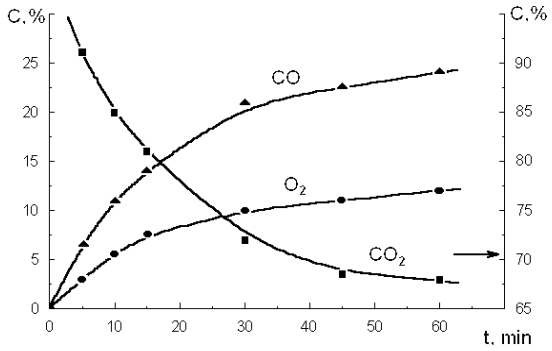


*Fig. 3. Time dependence of $CO$ and $O_2$ production.*

The maximum production of $CO$ from $CO_2$ attained 24.1% for an hour of work, and the percentage content of carbon dioxide decreased by 33%.

In the course of experiments, the following phenomenon was observed. Having determined the percentage content of products produced in $CO_2$ at a pressure of 1 atm. for 5, 10, 15 and 30 minutes, and having started the 45-minute run of production, suddenly, at the 35th minute of continuous burning of the discharge we observed an explosion in the reactor chamber, which was accompanied by a sonic effect, a flash of light in the whole volume of the reactor and an abrupt change in pressure in the chamber. The light flash was instantaneous, the gas pressure in the reactor quickly changed and the discharge continued burning. The mass-spectrogram that was taken at the time has revealed the fact of total burnout of carbon oxide in oxygen. An insignificant production of $CO$ (~ 2%) and $O_2$ (~1%) is apparently a result of a new production for the period from the explosion to the cutoff of the discharge.

Fig. 3 can be used to determine the critical values of components produced before the explosion ($CO(crit)$, $O_2(crit)$) and the percentage content of the initial product, i.e., carbon dioxide, at that time. The threshold pressure in the reactor directly before the explosion was determined from vacuum gauge readings. For the 35th minute of discharge burning the production of $CO$ was $CO(crit) \approx 21\%$, $O_2(crit) \approx 10\%$, reduction in $CO_2(crit) \approx 30\%$, gas pressure in the reactor $P_{crit} \approx 1.1$ atm (this being in agreement with theory - $\Delta P_{crit} \sim C/2$, where $C$ is the percentage content of $CO$).

The experimental results indicate that with the achievement of critical values, the instantaneous burnout of $CO$ in the $CO_2$ atmosphere proceeds in accordance with the chemical reaction [6]

$$2CO + O_2 \rightarrow 2CO_2, \quad \Delta H = -572 \text{ kJ/mole}$$

with a release of a great amount of energy.

Studies were also made of the discharge in $CO_2$ at a negative potential across the upper multi-needle electrode (the pressure in the reactor chamber P = 1 atm.). With the connected 220 pF capacitor, the spark frequency sometimes increased up to 3 kHz; however, in this case, one could observe a strong discharge instability accompanied by the transition to the arc discharge with a local burnout of the gas.

### 4.2 Experiments on $NO_x$ synthesis and $SO_x$ dissociation

The process of $NO_x$ synthesis from air and mixture of $N_2$ and $O_2$ at atmosphere pressure in PCR so as $SOx$ dissociation were investigated during multi-spark discharge at voltage 12-13 keV, current 80 A, pulsed duration 0.8 μs, repetition frequency 0.5-1.5 kHz. The content of $NO_x$ up to 10% was obtained. The methods of NO and $NO_2$ content determination in $NO_x$ were elaborated. The measurements of $NO_x$ removal by water evaporation was performed.

$SO_2$ was obtained in a special device by $S$ burning in gases mixture of 80% $O_2$ and 20% $Ar$. The value 22.7% of $SOx$ decrease was evaluated from the mass-spectra of initial mixture and treated one by the discharge during one hour. The dependence of separate contents decrease upon treatment duration is shown in Fig. 4.

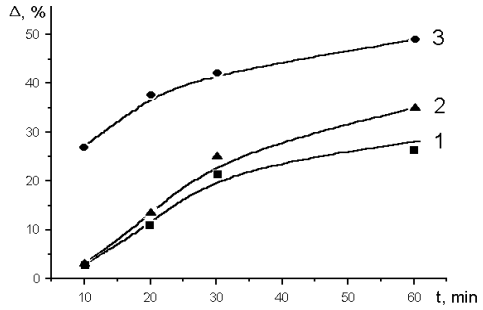


*Fig. 4 Dependence of $\Delta SO_2$(1), $\Delta SO$(2), $\Delta M_{32}$(3) on time*

The changes of pressure $\Delta P/P$=22.4% and temperature $\Delta T/T$=3.5% were observed So from pressure changing we can determine $SOx$ concentration decrease (i.e. $\Delta n/n \approx \Delta P/P$), that is coincident with mass-spectra data.

## 5. Discussion

Let us compare experimental results with theoretical estimations. The reactor parameters are: volume 3.5 l; interelectrode spacing (1.2 to 1.5)·10-2 m; discharge voltage 2 to 3 kV (arc discharge), up to 13 kV (corona and spark discharges); gas pressure in the chamber from 0 to 1.2 atm.; discharge currents 1 mA (corona discharge), 15 mA (arc discharge), tens of amperes (spark discharge).

### 5.1 Corona discharge

The average reduced electrical field is $E/N = 50$ Td = 12.5 kV/cm. As it was indicated the electron distribution function is such that the major portion of 2 to 3 eV electrons excites the vibrational levels so that $\langle \sigma v \rangle_{vib} \sim 6 \cdot 10^{-8}$ cm$^3$/s with the threshold $\Delta\varepsilon_{vib} = 8.2 \cdot 10^{-2}$ eV, and only a small their portion $\alpha$ leads to a direct dissociation of $CO_2$ molecules: $\langle \sigma v \rangle_{dis} \sim 5 \cdot 10^{-11}$ cm$^3$/s with the threshold energy $\Delta\varepsilon_{dis} = 5.5$ eV. The mean drift velocity of electrons is $v_d = 10^7$ cm/s. For the 2 mA current and a cone-shaped geometry of the discharge with the cross section of 0.5 cm$^2$ we find from (8) $n_e^* = 10^9$ cm$^{-3}$. Using (9) for the continuous mode of operation we find

$$k_1 = \sum n_e \langle \sigma_i v_i \rangle \approx \frac{\Delta\varepsilon_{vib}}{\Delta\varepsilon_{dis}} n_e^* \langle \sigma v \rangle_{vib} + a n_e^* \langle \sigma v \rangle_{dis} .$$

At $a \sim 0$, we find $k_1 = 1$.

From (24) we obtain the concentration at a maximum production $n_{CO}^{max} = 10^{17}$ cm$^{-3}$, i.e., $n_{CO}/n_{CO_2} \le 1\%$, and from (27) we find the saturation time $\tau_{CO} \sim 0.8$ μs.

### 5.2 Multi-spark discharge

For the same $E/N$ values in the case of a multi-spark discharge we have the pulsed current $I = 80$ A, the pulse duration $\tau = 0.5$ μs with the pulse repetition rate $f \sim 1$ kHz, the spark diameter $d = 1 \cdot 10^{-3}$ m, only one spark burning at each instant of the breakdown. From equation (8) we find that

$$j = \frac{I\tau f}{\pi d^2}, \qquad n_e = \frac{j}{e v_d} = 10^{12} \text{ cm}^{-3}.$$

So, from equation (9) we obtain the dissociation coefficient $k_1 = 10^3$.

From (24) and (27) we calculate the $CO$ concentration and the time of production

$$\frac{n_{CO}^{max}}{N_{CO_2}} = 30\%, \qquad \tau_{CO} \approx 30 \text{ μs}.$$

The shortest time of production in experiment was

$$\tau_2^{exp} = \tau_{CO} \frac{V}{\Delta V} \delta = 10^4 \text{ s}.$$

Here $V$ is the reactor volume, $\Delta V$ is the discharge region volume, $\delta$ is the pulse off-duty factor.

For the arc discharge and solitary spark discharges the production results are somewhat higher, though insignificantly.

The energy input per $CO_2$ dissociation event is defined as a ratio of the power brought into the discharge to the number of $CO_2$ molecules dissociated into the $CO$ molecules: $\varepsilon = W/N_{CO}$. For the multi-spark mode of operation at 20% of $CO$ production in $t = 30$ minutes, the number of $CO$ molecules will be $N_{CO} = C N_{CO_2} V = 0.2 \cdot 2.7 \cdot 10^{19} \cdot 3.5 \cdot 10^3 = 1.9 \cdot 10^{22}$.

Taking into account that the current pulse has the amplitude $I = 80$ A with a halfwidth $\tau = 0.5/2$ μs at a repetition rate $f = 1$ kHz, and the electrode voltage is $U = 12.5$ kV, we calculate the power brought into the discharge as $W = IU\tau ft = 2 \cdot 10^{24}$ eV. So, the discharge input power is $\varepsilon^{exp} = 100$ eV/mole.

## 6. References


1. Satoshi Sugimoto, Shunji Norikane, Atsushi Takehara, and Seiichi Goto. Operating Characteristics of a Glow Plasma Discharge at Atmospheric Pressure // Proc.1996 Int. Conf. On Plasma Physics, Nagoya, 1996
2. Vedenov A.A. Fizika electrorazryadnogo lazera // M. Energoizdat. 1982. 112 p (In Russian).
3. Kondratev V.N. Soobszenie po kinetike i katalizu 1979 V. 1 P. 7.
4. Ivanov Yu.A. Polak L.S., Slovetski D.I. Khimiya vysokich energij. 1971 V.5 P.382
5. .Napartovich A.P. et.al. A numerical simulation of Trichel-pulse formation in a negative corona. // J. Phys. D: Appl. Phys. 1997 V. 30. P. 2726.
6. Glinka N.L. Obschaya khimiya. // M.: "Khimiya", 1965. (In Russian).